

NONLINEAR VIBRATION ANALYSIS OF A HEAVY TRUCK DRIVER SEAT FOR DRIVER FATIGUE REDUCTION

Nuraj I. Rajapakse*
Graduate student

Gemunu S. Happawana
Assistant Professor

Department of Mechanical Engineering
Southern Methodist University, Dallas, TX 75275, USA

Keywords: Nonlinear modeling, Dynamic stability, Phase portrait, Roll angle, Seat vibration, Driver fatigue

Abstract

In this paper the driver seat vibration, leading to driver fatigue, of a heavy truck model is presented in a nonlinear framework. The model consists of a sprung mass, an unsprung mass, and a driver seat. All springs and dampers are considered nonlinear. An external force as a sudden impact on any of the truck-trailer wheels is used to analyze the vibrations of the seat to obtain information on the driver fatigue. The dynamic behavior of the driver seat including the sprung and unsprung masses is illustrated using parameters dependent phase portraits. This model is used in another paper by the same authors to implement a combined sliding mode and quantitative feedback controller to reduce the driver fatigue.

NOMENCLATURE

m_s	- Sprung mass of the i^{th} axle
m_u	- Unsprung mass related to the i^{th} axle
m_h	- Mass of the driver seat
F_h	- Nonlinear force of the driver seat
F_{s1}, F_{s2}	- Nonlinear spring and damper forces on the i^{th} axle
$F_{t1}, F_{t2}, F_{t3}, F_{t4}$	- Nonlinear tire forces of the i^{th} axle
k_s	- Nonlinear vertical stiffness of the suspension spring on the i^{th} axle
k_h	- Nonlinear vertical stiffness of the seat spring on the i^{th} axle
k_t	- Tire stiffness
J_s	- Roll inertia moment of the sprung mass related to i^{th} axle
J_u	- Roll inertia moment of the i^{th} axle
x_h	- Generalized coordinate of the driver seat on the i^{th} axle
x_s	- Generalized coordinate of the sprung mass on the i^{th} axle
x_u	- Generalized coordinate of the unsprung mass on the i^{th} axle
C_s	- Nonlinear damping coefficient of the suspension damper on the i^{th} axle
C_h	- Nonlinear damping coefficient of the seat damper on the i^{th} axle
C_t	- Tire damping
A_i	- Dual tire spacing per dual tires
S_i	- Half spacing between the suspensions on the i^{th} axle
T_i	- Half spacing between the inner tires
θ_s	- Roll angle of sprung mass.

θ_u - Roll angle of the i^{th} axle

* Corresponding Author

1. INTRODUCTION

Relationship between driver fatigue and seat vibration is used in literature based only on anecdotal evidence [1, 2]. It is widely believed and proved in field tests the lower vertical accelerations will increase comfort level of the driver [3-5]. Heavy truck drivers experiencing frequencies around 3 Hz could undergo driver fatigue and get drowsy, leading to road accidents [6]. Typically heavy truck drivers experience vibrations in the range 0.4 m/s^2 - 2.0 m/s^2 with a mean value of 0.7 m/s^2 in the vertical axis [3-6]. Intermittent and random vibration can have a stimulating or weakening effect on the driver. Body metabolism and chemistry can largely be changed due to this vibration exposure causing fatigue effects [7].

A suspension system that links the wheels to the vehicle body determines the ride comfort of the vehicle. Therefore its characteristics must be properly evaluated to design a driver seat under various vibration conditions. A properly designed driver seat can reduce the driver fatigue in riding against varying external disturbances.

The subject of improving the dynamic behavior of heavy trucks with higher-load capacity is an active area of research [8-14]. These heavy trucks are articulated vehicles consisting of standard highway triaxle tractors and one or more articulated units [8-12]. Usually the dynamic stability of the articulated vehicles is determined by the performance of each and every unit of the truck-trailer combination [15, 16]. There have been extensive researches to assess the dynamic performance, and to provide guidance in all its design stages [13, 14]. Critical oscillation frequencies, the lateral dynamic damping behavior of the truck-trailer combinations and their instabilities under extreme driving conditions are discussed [9]. The roll angle study shows that in field tests the roll motion not only alters other responses such as yaw, pitch etc. through suspension action but also has a significant effect on the directional dynamic behavior of these trucks [8].

In general, the suspension springs and the dampers are inherently nonlinear and the linear equations cannot be used to predict the actual physical behavior of these vehicles. The linear analytical techniques are useful and provide simplified solutions to many vehicle dynamics problems [10]. However, critical truck oscillating frequencies, damping action of the oscillating system, and instabilities under extreme driving conditions may not be properly discussed by the application of linear equations. Stability of equilibrium points may change from stable to unstable or vice versa by varying the parameters of a truck [11].

In this paper, a nonlinear five degree-of-freedom mathematical model of a heavy truck drive seat is developed by considering an axle unit that undergoes a sudden impact on any of its wheels. The transmission of vibrations to the driver seat of the truck due to road disturbances is investigated. The analysis in this paper may easily be extended to multiple axle truck-trailer combinations, with increasing number of degrees of freedom depending on the number of axles.

2. MATHEMATICAL MODELING

Figures 1 and 2 show schematic of a five degree-of-freedom truck axle unit and its roll motion configuration with the driver seat in the sprung mass. The model is consisting of a sprung mass, an unsprung mass (axle and tires), suspensions and a driver seat. Furthermore, all

the springs and dampers are assumed to remain parallel to the vertical axis and transmit only compressive and tensile forces. The model allows the sprung and the unsprung masses to roll nonlinearly with a presence of a disturbance to any tire of the axle. In the analysis, it is assumed that the tires attached to the same axle are identical in stiffness and damping coefficients. Moreover, it is considered that the driver seat and the sprung mass have the same roll angle.

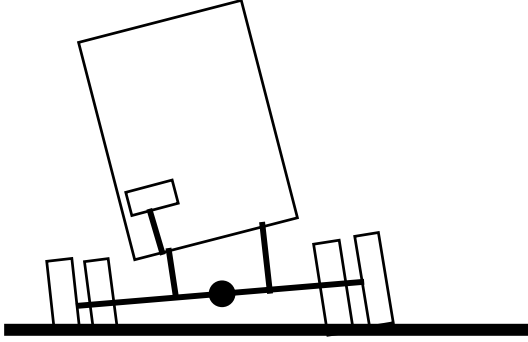


Fig. 1: The schematic of a five-degree-of-freedom nonlinear roll and bounce model of a truck driver seat

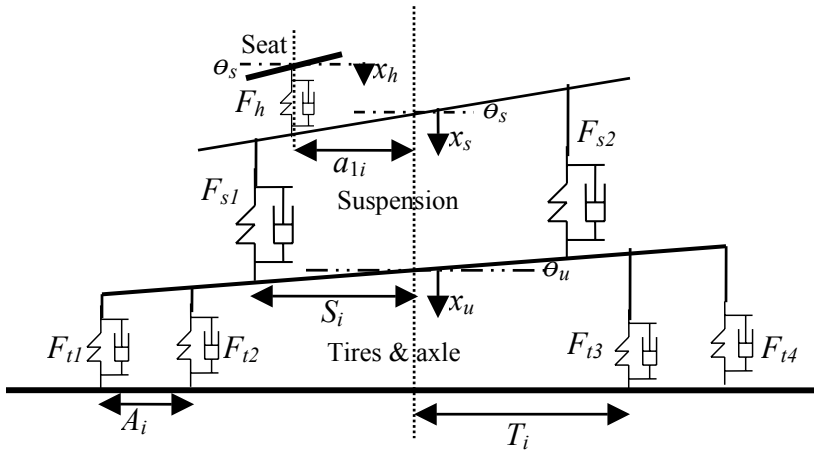


Fig. 2: Five-degree-of-freedom roll and bounce motion configuration of the system to a sudden impact

3. MODELING OF NONLINEAR STIFFNESS AND DAMPING

The spring forces of the linear and the nonlinear stiffness modeling [17, 19] are as follows:

$$F_{spring} = k_i l \rightarrow \text{linear}$$

$$F_{damper} = C_i \dot{l} \rightarrow \text{linear}$$

$$F_{spring} = k_{i1} l + k_{i2} l^3 \rightarrow \text{nonlinear with 1 nonlinear term}$$

$$F_{spring} = k_{i1} l + k_{i2} l^3 + k_{i3} l^5 \rightarrow \text{nonlinear with 2 nonlinear terms}$$

$$F_{dampner} = C_{i1}\dot{l} + C_{i2}|\dot{l}|^2 \dot{l} \rightarrow \text{nonlinear with 1 nonlinear term}$$

$$F_{dampner} = C_{i1}\dot{l} + C_{i2}|\dot{l}|^2 \dot{l} + C_{i3}|\dot{l}|^4 \dot{l} \rightarrow \text{nonlinear with 2 nonlinear terms}$$

Where

l is the deflection of the spring in meters

\dot{l} is the time derivative of l , $\frac{dl}{dt}$

$k_i, C_i, k_{i1}, k_{i2}, k_{i3}, C_{i1}, C_{i2}, C_{i3}$ are constants

In general, spring and damper forces given by the linear equations do not represent true dynamics of the system, specially for larger deflections. This can be avoided by adding appropriate nonlinear terms into linear equations for spring and damper forces. Figure 3 and Fig. 4 show the differences in using linear and nonlinear terms as arranged in the following equations, where r_{i1}, r_{i2}, q_{i1} , and q_{i2} have unit magnitudes.

$$F_{spring} = k_{i1}(l + r_{i1}l^3)$$

$$F_{spring} = k_{i1}(l + r_{i1}l^3 + r_{i2}l^5)$$

$$F_{dampner} = C_{i1}(\dot{l} + q_{i1}|\dot{l}|^2 \dot{l})$$

$$F_{dampner} = C_{i1}(\dot{l} + q_{i1}|\dot{l}|^2 \dot{l} + q_{i2}|\dot{l}|^4 \dot{l})$$

Where

$r_{i1} = k_{i2}/k_{i1}$ and $r_{i2} = k_{i3}/k_{i1}$ – Relative Spring Constants

$q_{i1} = C_{i2}/C_{i1}$ and $q_{i2} = C_{i3}/C_{i1}$ – Relative Damping Coefficients

It is evident from the graphs that the linear equations can be used accurately only for small deflections and small velocities, where as nonlinear equations can cover a wide range of values. Furthermore, adding higher order nonlinear terms can accurately represent the dynamics of the system. However, as shown in Fig. 3 and Fig. 4, the curves are fairly close to each other for single and multiple nonlinear terms. It can be concluded that the above nonlinear equation with one nonlinear term can satisfactorily represent the actual dynamics of the system.

It is very important to mention that relative spring and damping coefficients are not equal to one always. It is dependent upon various factors and can be checked experimentally before doing the analysis. For certain springs that have been checked in our laboratory, above values are found to be true in a wide range of operating conditions. Furthermore, one can think of above nonlinear terms in a different way by using variable functions for deflection and rate of change of deflection as follows:

$$F_{spring} = (k_{i1} + k_{i2}l^2 + k_{i3}l^4)l$$

$$F_{spring} = K_l l$$

$$F_{dampner} = (C_{i1} + C_{i2}|\dot{l}|^2 + C_{i3}|\dot{l}|^4)\dot{l}$$

$$F_{dampner} = C_l \dot{l}$$

Where

$$K_l = f(l) \text{ and } C_l = f(\dot{l})$$

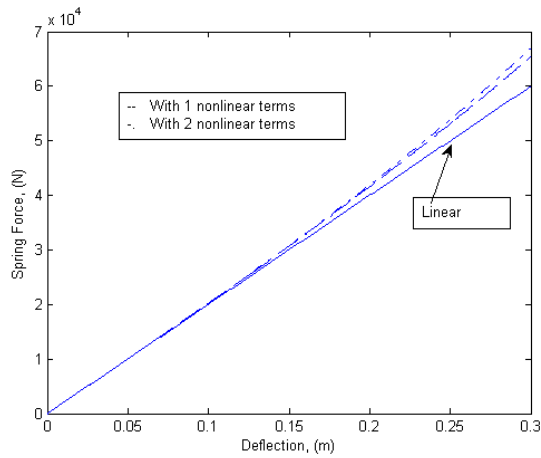


Fig. 3: The linear and the nonlinear spring deflection vs. spring force

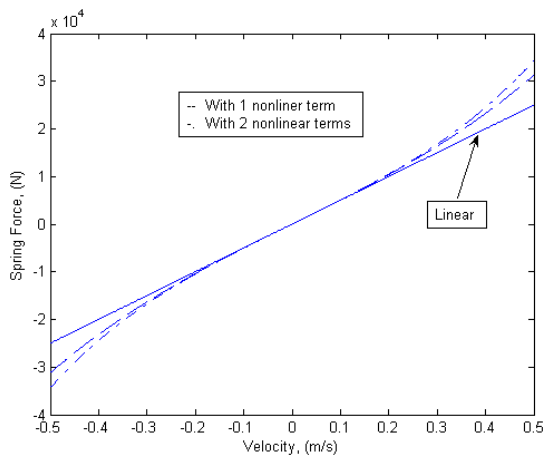


Fig. 4: The velocity vs. damping force for linear and the nonlinear cases

4. COMMON EQUATION FOR REPRESENTING NONLINEAR FORCE

Nonlinear tire forces, suspension forces, and driver seat forces can be obtained by substituting appropriate coefficients to the following nonlinear equation that covers wide range of operating conditions for representing dynamical behavior of the system.

$$F = k(d + d^3) + C(1 + |\dot{d}|^2)\dot{d}$$

Where

F – Force

k – Spring constant

C – Damping coefficient

d – Deflection

\dot{d} – Rate of change of deflection

For the suspension:

$$F_{si} = k_{si}(d_{si} + d_{si}^3) + C_{si}(1 + |\dot{d}_{si}|^2)\dot{d}_{si}, \quad i = 1, 2$$

For the tires:

$$F_{ti} = k_{ti}(d_{ti} + d_{ti}^3) + C_{ti}(1 + |\dot{d}_{ti}|^2)\dot{d}_{ti}, \quad i = 1, 2, 3, 4$$

For the seat:

$$F_h = k_h(d_h + d_h^3) + C_h(1 + |\dot{d}_h|^2)\dot{d}_h$$

5. DEFLECTION OF THE SUSPENSION SPRINGS AND DAMPERS

Based on the mathematical model developed, deflection of the suspension system on the axle is found for both sides as follows:

$$\text{Deflection of side 1, } d_{s1} = (x_s - x_u) + S_i(\sin \theta_s - \sin \theta_u)$$

$$\text{Deflection of side 2, } d_{s2} = (x_s - x_u) - S_i(\sin \theta_s - \sin \theta_u)$$

6. DEFLECTION OF THE SEAT SPRINGS AND DAMPERS

By considering the free body diagram in Fig. 2, deflection of the seat is obtained as follows:

$$d_h = (x_h - x_s) - a_{1i} \sin \theta_s$$

7. TIRE DEFLECTIONS

The tires are modeled by using springs and dampers. Deflections of the tires to a road disturbance are given by the following equations.

$$\text{Deflection of tire 1, } d_{t1} = x_u + (T_i + A_i) \sin \theta_u$$

$$\text{Deflection of tire 2, } d_{t2} = x_u + T_i \sin \theta_u$$

$$\text{Deflection of tire 3, } d_{t3} = x_u - T_i \sin \theta_u$$

$$\text{Deflection of tire 4, } d_{t4} = x_u - (T_i + A_i) \sin \theta_u$$

8. EQUATIONS OF MOTION

Based on the mathematical model developed above, the equations of motion for each of the sprung mass, unsprung mass, and the seat are written by utilizing the free-body diagram of the system in Fig. 2 as follows:

Vertical and roll motion for the i^{th} axle (unsprung mass)

$$m_u \ddot{x}_u = (F_{s1} + F_{s2}) - (F_{t1} + F_{t2} + F_{t3} + F_{t4}) \quad (1)$$

$$J_u \ddot{\theta}_u = S_i (F_{s1} - F_{s2}) \cos \theta_u + T_i (F_{t3} - F_{t2}) \cos \theta_u + (T_i + A_i) (F_{t4} - F_{t1}) \cos \theta_u \quad (2)$$

Vertical and roll motion for the sprung mass

$$m_s \ddot{x}_s = -(F_{s1} + F_{s2}) + F_h \quad (3)$$

$$J_s \ddot{\theta}_s = S_i (F_{s2} - F_{s1}) \cos \theta_s + a_{1i} F_h \cos \theta_s \quad (4)$$

Vertical motion for the seat

$$m_h \ddot{x}_h = -F_h \quad (5)$$

Equations (1)-(5) have to be solved simultaneously, since there exist many parameters and nonlinearities. Nonlinear effects can better be understood by varying the parameters and examining relevant dynamical behavior, since changes in parameters change the dynamics of the system. Furthermore, Equations (1)-(5) can be represented in the phase plane, while varying the parameters of the truck, since each and every trajectory in the phase portrait characterizes the state of the truck. Equations above can be converted to the state space form and the solutions can be obtained using MATLAB as below. Phase portraits are used to observe the nonlinear effects with the change of the parameters. Change of initial conditions clearly changes the phase portraits and the important effects on the dynamical behavior of the truck can be understood. The following symbols are used for the MATLAB program.

$$x(1) = x_u, \quad x(2) = \dot{x}_u, \quad x(3) = x_s, \quad x(4) = \dot{x}_s, \quad x(5) = x_h, \quad x(6) = \dot{x}_h, \quad x(7) = \theta_u, \quad x(8) = \dot{\theta}_u, \\ x(9) = \theta_s, \quad x(10) = \dot{\theta}_s$$

9. SIMULATION AND RESULTS

Different initial conditions can be selected for the simulation by considering various parameters such as steer angle, a sudden bump on the road and the change in road surface etc. Most of the cases among them result in either a change in vertical displacement or roll angle of the unsprung mass. The phase portraits and time graphs are drawn with an initial vertical displacement, velocity, roll angle, and roll rate of the unsprung mass for 0.3 m, 0.3m/s, 0.3 rad, and 3 rad/s, which can represent sudden impact on any wheel. The corresponding sprung mass initial conditions are 0.2 m, 0.2m/s, 0.2 rad, and 2 rad/s. Initial conditions for the driver seat vertical displacement and velocity are selected as 0.1 m and .1m/s. It is very important to mention that these initial conditions are particularly selected to examine the impulsive response on the truck dynamics. Slight change of initial conditions will change the phase portrait and result in qualitatively different dynamic stability. Furthermore, differences on the dynamical behavior of the truck with respect to linear and nonlinear equations are clearly shown in most of the phase portraits. The tire spring constant values and the tire damping coefficients change the

phase portrait and the reach of stability which indeed be used for selecting suitable parameters to reduce driver fatigue and vibrations.

Linear Analysis:

Small angle approximations can be used to obtain the linearized equations and they are as follows:

Assume θ_u & θ_s are very small ($\theta_s > \theta_u$) to obtain the following approximations.

$\sin \theta_u = \theta_u$, $\cos \theta_u = 1$, $\sin \theta_s = \theta_s$ and $\cos \theta_s = 1$.

Vertical and roll motion for the i^{th} axle (unsprung mass)

$$m_u \ddot{x}_u = 2k_s(x_s - x_u) + 2C_s(\dot{x}_s - \dot{x}_u) - 4k_t x_u - 4C_t \dot{x}_u \quad (6)$$

$$J_u \ddot{\theta}_u = 2k_s S_i^2(\theta_s - \theta_u) + 2C_s S_i^2(\dot{\theta}_s - \dot{\theta}_u) - 2k_t T_i^2 \theta_u - 2C_t T_i^2 \dot{\theta}_u - 2k_t(T_i + A_i)^2 \theta_u - 2C_t(T_i + A_i)^2 \dot{\theta}_u \quad (7)$$

Vertical and roll motion for the sprung mass

$$m_s \ddot{x}_s = -2k_s(x_s - x_u) - 2C_s(\dot{x}_s - \dot{x}_u) + k_h(x_h - x_s) - k_h a_{1i} \theta_s + C_h(\dot{x}_h - \dot{x}_s) - C_h a_{1i} \dot{\theta}_s \quad (8)$$

$$J_s \ddot{\theta}_s = -2k_s S_i^2(\theta_s - \theta_u) - 2C_s S_i^2(\dot{\theta}_s - \dot{\theta}_u) + k_h a_{1i}(x_h - x_s) - k_h a_{1i}^2 \theta_s + C_h a_{1i}(\dot{x}_h - \dot{x}_s) - C_h a_{1i}^2 \dot{\theta}_s \quad (9)$$

Vertical motion for the seat

$$m_h \ddot{x}_h = -k_h(x_h - x_s) + k_h a_{1i} \theta_s - C_h(\dot{x}_h - \dot{x}_s) + C_h a_{1i} \dot{\theta}_s \quad (10)$$

In subsequent results, the spring constant of the tires is selected as 1200kN/m and the damping coefficient as 300kNs/m. Some of the trucks' numerical parameters [8, 12] are used in obtaining plots and they are listed below:

$m_h=100\text{kg}$, $m_s=3300\text{kg}$, $m_u=1000\text{kg}$, $k_s = 200 \text{ kN/m}$, $k_h = 1 \text{ kN/m}$, $C_s = 50 \text{ kNs/m}$, $C_h = 0.4 \text{ kNs/m}$, $J_s = 3000 \text{ kgm}^2$, $J_u = 900 \text{ kgm}^2$, $A_i = 0.3 \text{ m}$, $S_i=0.9 \text{ m}$, and $a_{1i} = 0.8 \text{ m}$.

Figures 5-14 reveal some of the changes of the linear and the nonlinear analysis. Figures 5, 6, 11, and 12 show the change of vertical and roll angle of the unsprung mass for both the linear and nonlinear cases. Qualitatively, linear and nonlinear analysis show excellent agreement on the vertical displacement and roll angle of the unsprung mass. Figures 7, 8, 13, and 14 are obtained for sprung mass vertical displacement and roll angle behavior. Many of the neglected terms of the linear analysis under predict the vertical displacement and roll angle of the sprung and unsprung masses than the nonlinear analysis resulting inaccurate predictions.

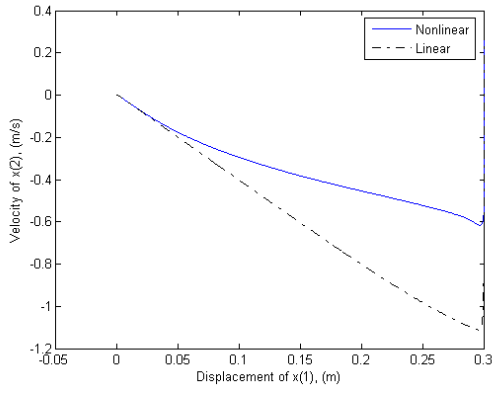


Fig. 5: Phase portrait for the change of displacement vs. the velocity of the unsprung mass vertical motion

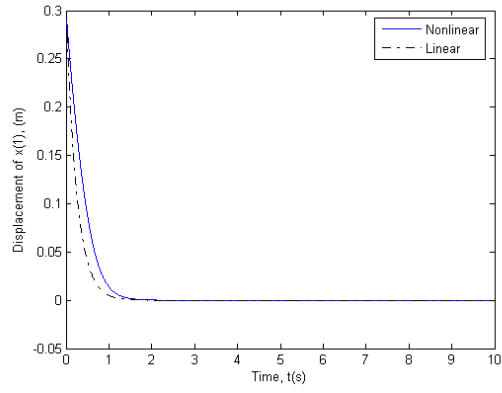


Fig. 6: Vertical displacement of the unsprung mass vs. time

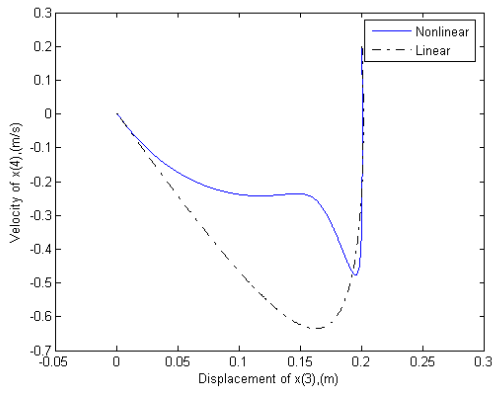


Fig. 7: Phase portrait for the change of displacement vs. the velocity of the sprung mass vertical motion

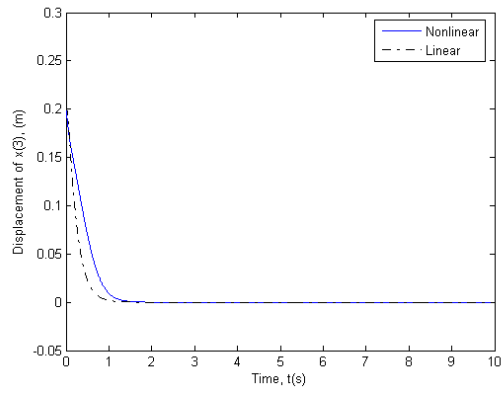


Fig. 8: Vertical displacement of the sprung mass vs. time

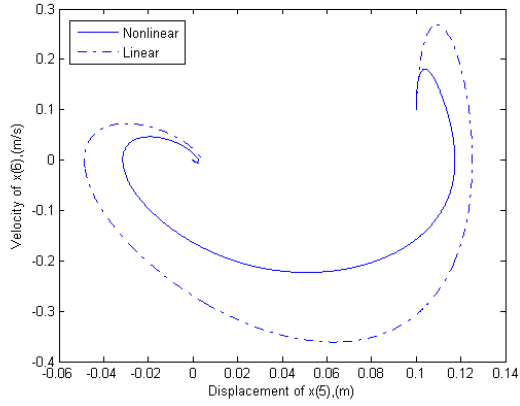


Fig. 9: Phase portrait for the change of displacement vs. the velocity of the driver seat vertical motion

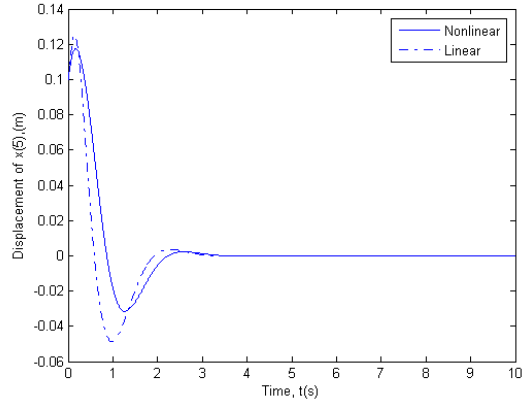


Fig. 10: Vertical displacement of the driver seat vs. time

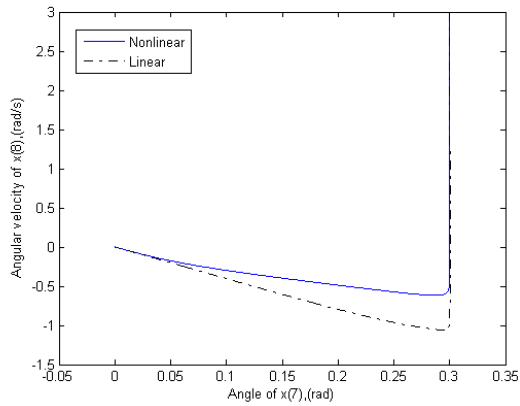


Fig. 11: Phase portrait for the change of angle vs. the angular velocity of the unsprung mass roll motion

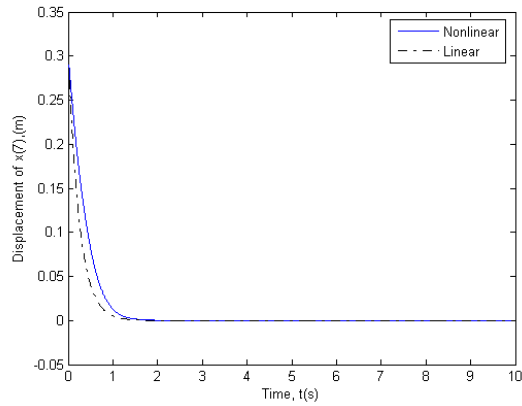


Fig. 12: Change of angle of the unsprung mass roll motion vs. time

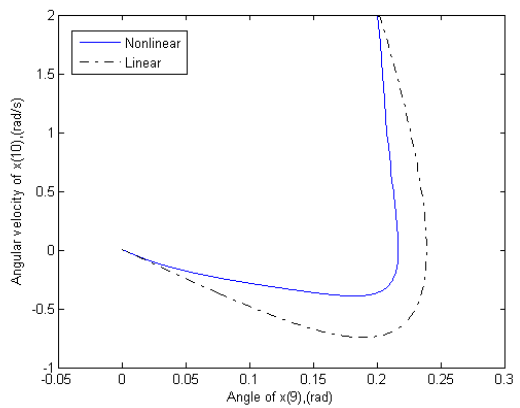


Fig. 13: Phase portrait for the change of angle vs. the angular velocity of the sprung mass roll motion

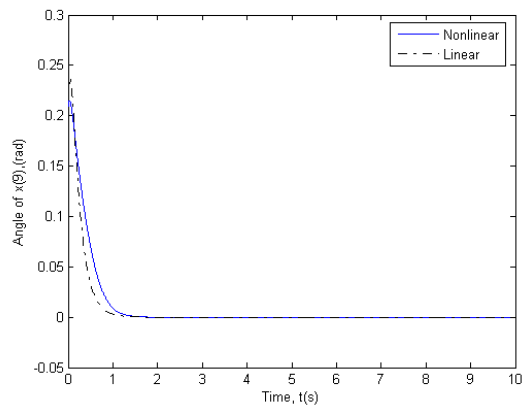


Fig. 14: Change of angle of the sprung mass roll motion vs. time

There is a significant variation in the transient behavior of the driver seat vertical displacement in linear and nonlinear analysis as shown in Figures 9 and 10. Change in dynamics due the variation of damping and stiffness coefficients for both the tire and the seat are illustrated from Fig. 15 to 22 by using the nonlinear system of equations.

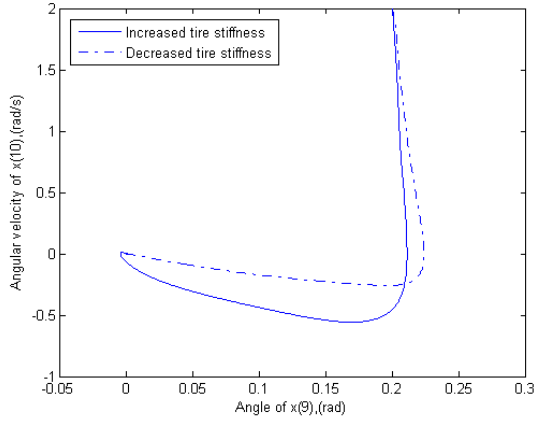


Fig. 15: Phase portrait for the change of angle vs. the angular velocity of the sprung mass roll motion for $k_t = 2400$ and 600 kN/m

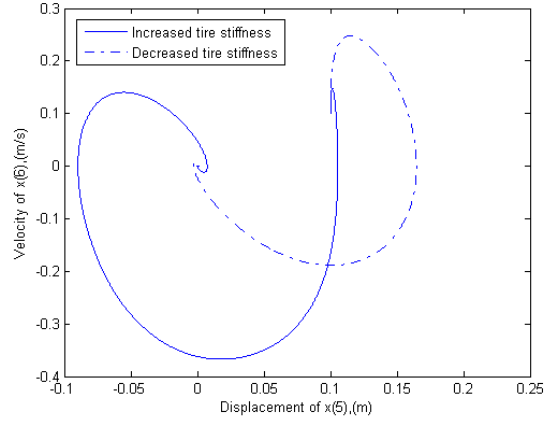


Fig. 16: Phase portrait for the change of displacement vs. the velocity of the driver seat vertical motion for $k_t = 2400$ and 600 kN/m

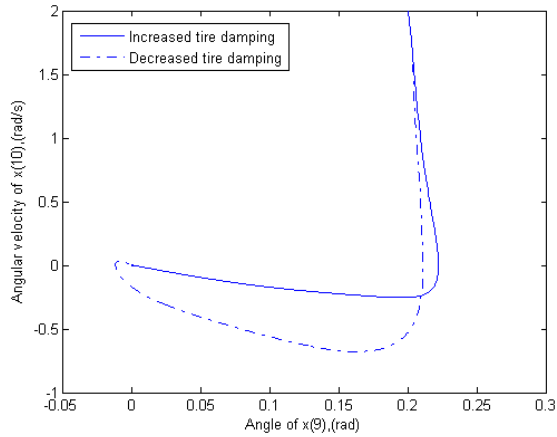


Fig. 17: Phase portrait for the change of angle vs. the angular velocity of the sprung mass roll motion for $C_t = 600$ and 100 kNs/m

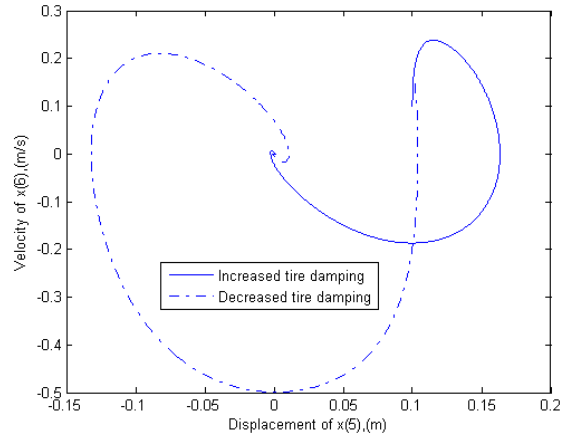


Fig. 18: Phase portrait for the change of displacement vs. the velocity of the driver seat vertical motion for $C_t = 600$ and 100 kNs/m

Figures 15-18 show the change in dynamics of the driver seat for two different tire stiffness and damping coefficients. Solid lines give the phase portraits for higher stiffness and damping coefficients, whereas dash lines give the phase portraits for lower stiffness and damping coefficients. Reduction of tire spring constant increases the roll angle of the driver seat where as decrease in tire damping increases the roll angle as shown in Fig. 15 and Fig. 17. Figures 16 and 18 reveal noticeable change in dynamics of the driver seat vertical displacement for different tire stiffness and damping coefficients.

It is very important to mention that the change in values of the suspension spring stiffness and damping coefficient generates qualitatively different phase portraits in which higher values of suspension spring stiffness and damping coefficients result in decreased roll angle and displacement of the driver seat. Driver seat vibration is partly affected by the selection of the springs and dampers of the suspension system and the condition of the tires. Furthermore, tires must be carefully chosen in the valid range of design values and the suitable inflation pressure should be maintained at all times to operate at the right frequency limits to reduce driver fatigue. Phase portraits for sprung mass and driver seat roll motions are given with the assumption that the driver seat roll angle and the sprung mass roll angle are equal. These figures exhibit the qualitative couple dynamics for various spring and damping coefficients.

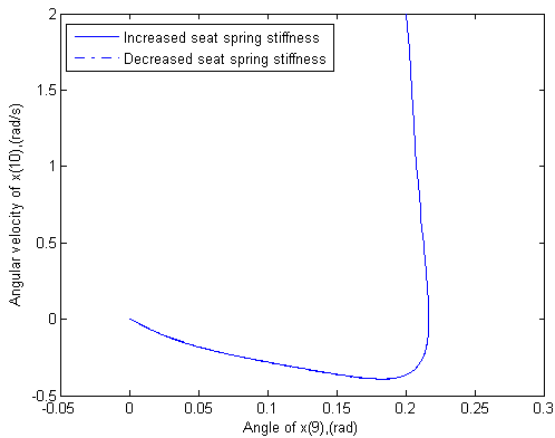


Fig. 19: Phase portrait for the change of angle vs. the angular velocity of the sprung mass roll motion for $k_h=2$ and 0.5 kN/m

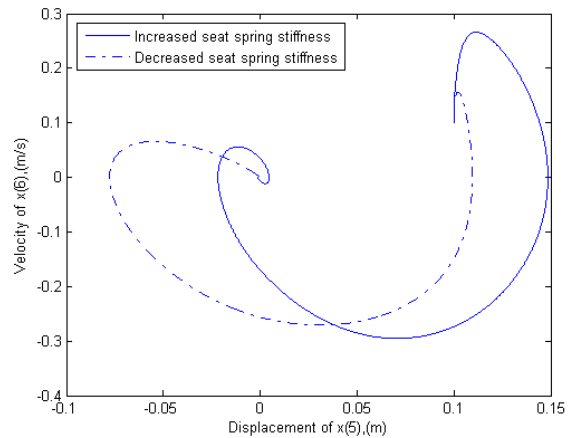


Fig. 20: Phase portrait for the change of displacement vs. the velocity of the driver seat vertical motion for $k_h=2$ and 0.5 kN/m

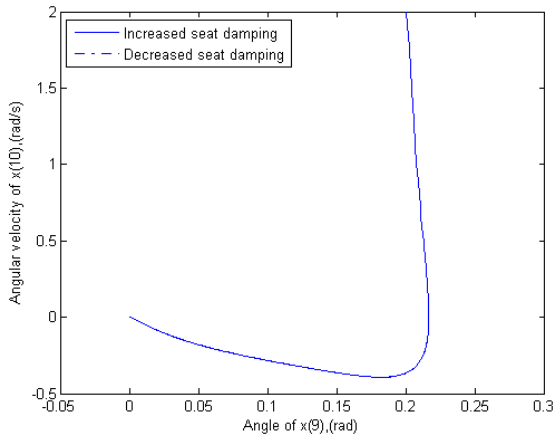


Fig. 21: Phase portrait for the change of angle vs. the angular velocity of the sprung mass roll motion for $C_h=1$ and 0.1 kNs/m

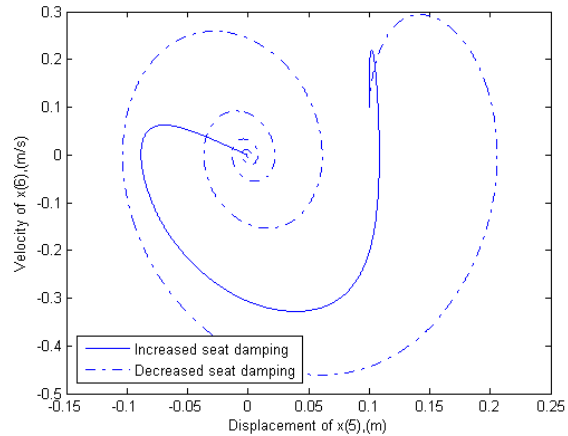


Fig. 22: Phase portrait for the change of displacement vs. the velocity of the driver seat vertical motion for $C_h=1$ and 0.1 kNs/m

Driver seat stiffness and damping coefficients are playing a major role in reducing driver fatigue. Increased seat spring stiffness and decreased damping coefficient will bring the system into steady state slower than the decreased stiffness and increased damping, leading to driver fatigue as shown in Figures 19 - 22. Figure 22 shows the phase portraits for seat vertical behavior. By reducing seat stiffness and increasing seat damping vibrations can be minimized and the areas of driver fatigue can effectively be addressed. In Figures 19 and 21, dash lines and solid lines are on top of each other representing sprung mass and driver seat roll dynamics are independent on the values of the seat spring stiffness and damping coefficients. That is in agreement with the assumption that the sprung mass and the driver seat have the same roll angle.

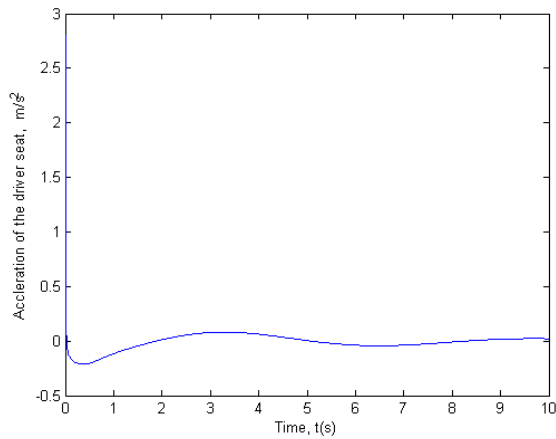


Fig. 23: Vertical acceleration of the driver seat vs. time for $k_h=100$ N/m and $C_h=40$ Ns/m

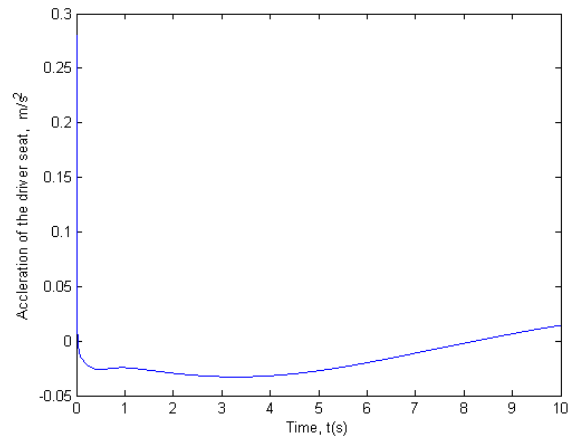


Fig. 24: Vertical acceleration of the driver seat vs. time for $k_h=10$ N/m and $C_h=4$ Ns/m

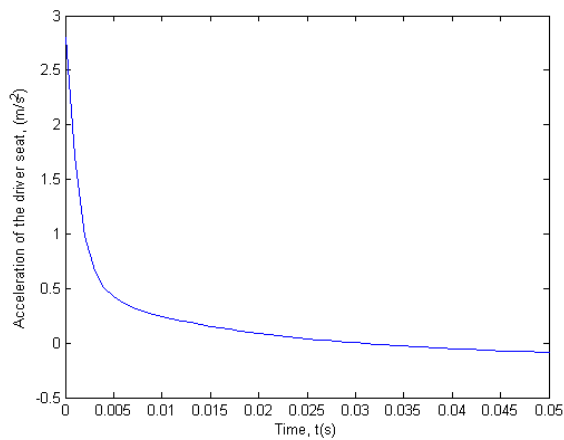


Fig. 25: Zoomed in vertical acceleration of the driver seat vs. time for $k_h=100$ N/m and $C_h=40$ Ns/m in the first 0.05 seconds

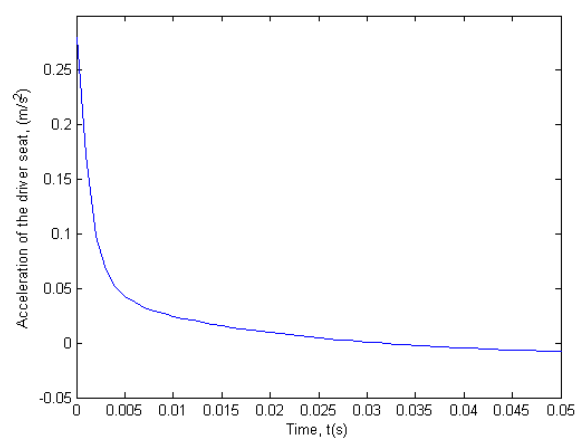


Fig. 26: Zoomed in vertical acceleration of the driver seat vs. time for $k_h=10$ N/m and $C_h=4$ Ns/m in the first 0.05 seconds

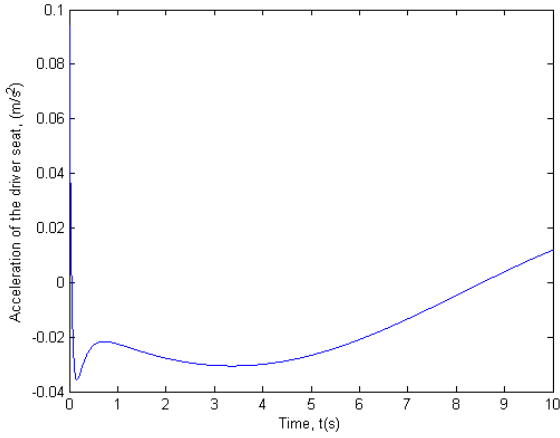


Fig. 27: Linear vertical acceleration of the driver seat vs. time for $k_h=10$ N/m and $C_h=4$ Ns/m

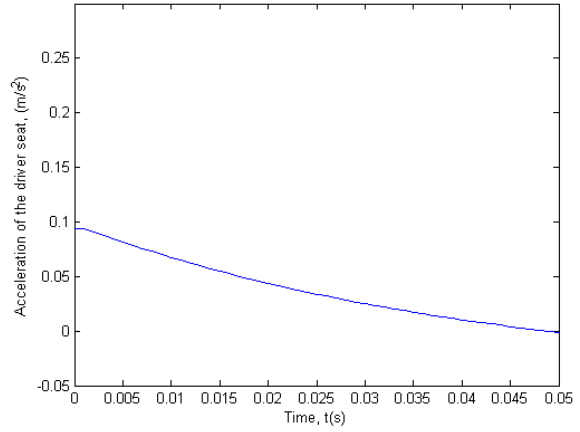


Fig. 28: Zoomed in linear vertical acceleration of the driver seat vs. time for $k_h=10$ N/m and $C_h=4$ Ns/m in the first 0.05 seconds

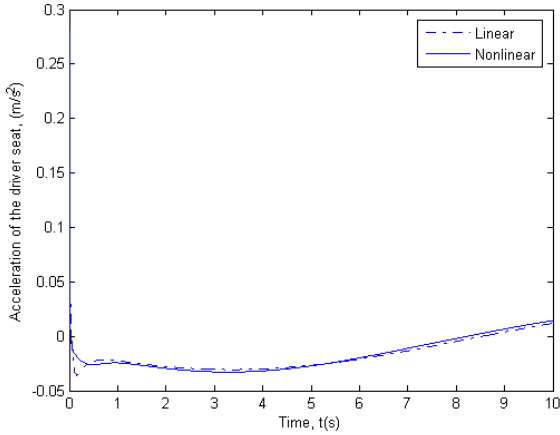


Fig. 29: Linear and nonlinear vertical acceleration of the driver seat vs. time for $k_h=10$ N/m and $C_h=4$ Ns/m

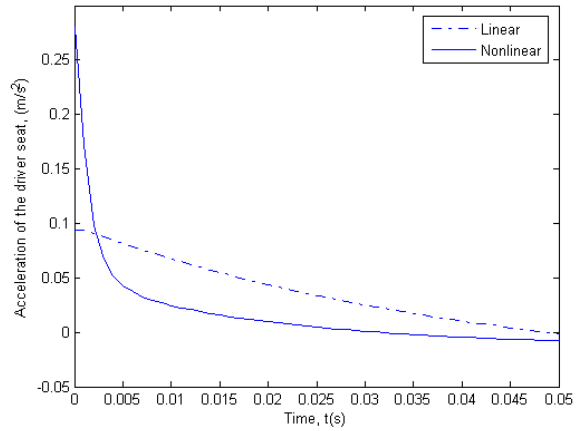


Fig. 30: Zoomed in linear and nonlinear vertical acceleration of the driver seat vs. time for $k_h=10$ N/m and $C_h=4$ Ns/m in the first 0.05 seconds

Figures 23-30 represent the time response of the vertical acceleration of the driver seat for two different seat stiffness and damping coefficient values. Figures 25 and 26 show the zoomed in vertical acceleration of the figures 23 and 24 in the first 0.05 seconds to clearly see the initial dynamical behavior. Figure 27 gives the initial vertical acceleration of the driver seat for the linear model and it is enlarged in Fig. 28 in the first 0.05 seconds. Figure 29 and Fig. 30 show the difference in using linear and nonlinear models to predict the vertical acceleration of the driver seat respectively. It is very important to mention here that the linear model under predicts the vertical acceleration of the driver seat than the nonlinear model. Reduction in seat stiffness and damping coefficients decreases vertical acceleration considerably. But it increases the seat deflection that can cause to reach seat deflection limits eventually. Therefore, it is a trade-off between reducing the vertical acceleration to reduce the driver fatigue while limiting the vertical deflection to avoid excessive seat travel. This study can effectively be used to analyze the performance of the driver seat for different vehicle system parameters with a view of reducing the driver fatigue.

It is worthwhile to mention that in order to reduce oscillatory behavior of the seat and to reduce the driver fatigue not only the seat construction, but also the other factors, i.e. tires and the suspension system, must carefully be examined to select the proper springs and dampers in the valid range of operation as shown in figures 15-18.

Actual dynamics of the system may not be predicted by using linear equations. The nonlinear equations must be used, as the forces and the reactions of a heavy truck can change within huge limits due to cargo loading. For this type of force change, springs and dampers behave in a nonlinear manner as defined in earlier sections. Furthermore, realistic dynamical models are required to design the controllers in a wide range of forces and deflections under various external disturbances. It can be concluded that the above nonlinear analysis would be helpful in many ways to design and analyze the driver seat of a heavy vehicle to minimize driver fatigue and to improve its performance.

10. CONCLUSIONS

A nonlinear mathematical roll model has been developed for a heavy trucks' axle unit with a driver seat in the sprung mass. As shown in above figures, the nonlinear results show some significant changes from the linear results. Nonlinear parameter effects can be used in obtaining displacements and angles of the sprung mass, unsprung mass, and driver seat for improved directional stability. Furthermore, the phase portraits for both the situations: linear and nonlinear, provide sufficient information that may be used to improve the handling and maneuverability. One of the fundamental advantages of this approach is to analyze the dynamic stability of the driver seat for varying system parameters with a view of reducing driver fatigue. Moreover, vertical acceleration of the driver seat can be maintained within a comfortable limit by changing the system parameters, mainly stiffness and damping coefficients of the driver seat.

Properties of tires and their operating conditions are very important in order to reduce seat oscillatory behavior. Proper selection of suspension springs and dampers minimizes seat vibrations. To design a proper controllable driver seat of a truck, actual physical behavior of the components of the seat must be taken into account. Information sources, i.e., sensors, actuators etc. to the main control unit can be selected in the valid ranges and this will lead to gathering precise dynamic information. In addition, the analysis provides initial steps in designing a controllable driver seat that reduces vibrations and driver fatigue in the actual nonlinear frame itself.

11. REFERENCES

- [1] Wilson, L. J. and Horner, T. W., 1979 " Data Analysis of Tractor-Trailer Drivers to Assess Drivers' Perception of Heavy Duty Truck Ride Quality ", Report DOT-HS-805-139, National Technical Information Service, Springfield, VA, USA.
- [2] Randall, J. M., 1992 " Human subjective response to lorry vibration: implications for farm animal transport " , J. Agric. Engng, Res, Vol 52, pp. 295-307.
- [3] Landstrom, U. and Landstrom, R., 1985 " Changes in wakefulness during exposure to whole body vibration " , Electroencephal, Clin, Neurophysiol, Vol 61, pp. 411-415.
- [4] Altunel, A.O., 1996 " The effect of low-tire pressure on the performance of forest products transportation vehicles " , Master's thesis, Louisiana State University, School of Forestry, Wildlife and Fisheries.

- [5] Altunel, A.O. and Hoop C. F. de, 1998 “ The Effect of Lowered Tire Pressure on a Log Truck Driver Seat ”, Louisiana State University Agric. Center, Baton Rouge, USA, Vol. 9, no. 2.
- [6] Mabbott, N., foster, G. and Mcphee, B. 2001, “ Heavy Vehicle Seat Vibration and Driver Fatigue ”, Australian Transport Safety Bureau, Report No. CR 203, pp. 35.
- [7] Kamenskii, Y. and Nosova, I. M., 1989 “ Effect of whole body vibration on certain indicators of neuro-endocrine processes ”, Noise and Vibration Bulletin, pp. 205-206.
- [8] Tabarrok, B. and Tong, X., 1993 “ Directional Stability Analysis of Logging Trucks by a Yaw Roll Model ”, Technical Reports, University of Victoria, Mechanical Engineering Department, pp. 57- 62
- [9] Pflug, H. –Chr., 1986 “ Lateral Dynamic Behaviour of truck-trailer Combinations due to the influence of the load ”, Vehicle Systems Dynamics, Vol. 15, pp. 155 – 175.
- [10] Esmailzadeh, E., Tong, L. and Tabarrok, B. 1990, “ Road Vehicle Dynamics of Log Hauling Combination Trucks ”, SAE Technical Paper Series 912670, pp. 453-466.
- [11] Chen, B. C. and Peng, H., 1999, “ Rollover Warning of Articulated Vehicles Based on a Time-to-Rollover Metric ”, Technical Reports, University of Michigan, Mechanical Engineering and Applied Science Department.
- [12] Tabarrok, B. and Tong, L., 1992, “ The Directional Stability Analysis of Log Hauling Truck – Double Doglogger ”, Technical Reports, University of Victoria, Mechanical Engineering Department, DSC-Vol 44, pp. 383-396.
- [13] Aksionov, P.V., 2001, “ Law and criterion for evaluation of optimum power distribution to vehicle wheels ”, Int. J. Vehicle Design, Vol. 25, No. 3, pp. 198-202.
- [14] Vladimir, V. V, Vysotski, M. S., Gileles, L. K., Zakharik, A. M., Happawana, G. S. and Nwokah, O. D. I., 2001, “ Optimization of mass and geometric vehicle parameters for multiple drive wheel trucks ”, Int. J. Vehicle Design, Vol. 25, No.3, pp. 170-181.
- [15] Wong, J. Y., 1978, Theory of Ground Vehicles, New York, N.Y., John Wiley and Sons.
- [16] Gillespie, T. D., 1992, Fundamentals of Vehicle Dynamics, SAE, Inc. Warrendale, PA.
- [17] Singiresu, S. R., 1986, Mechanical Vibrations, Addison-Wesley Publishing Company, Inc.
- [18] Strogatz, S. H., 1994, Nonlinear Dynamics and Chaos, Perseus Books Publishing, L.L.C.
- [19] Jean-Jacques, E. S. and Weiping, L., 1991, Applied Nonlinear Control, Prentice-Hall, Inc., Englewood Cliffs, New Jersey 07632.